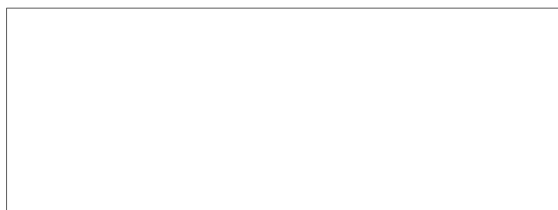STAT

STAT

TECHNICAL AND SCIENTIFIC SERVICES

IN

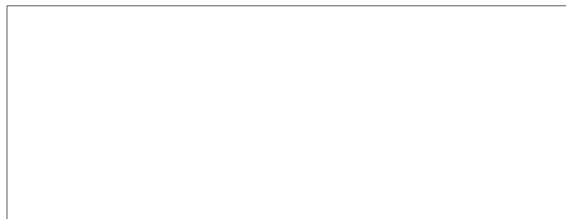GEOMETRICAL AND PHYSICAL OPTICS

Submitted by

STAT

15 June 1967

TECHNICAL PROPOSAL

TECHNICAL AND SCIENTIFIC SERVICES

IN

GEOMETRICAL AND PHYSICAL OPTICS

STAT

It is requested that the data set forth
herein shall not be disclosed outside the Govern-
ment or be duplicated, used or disclosed in whole
or in part for any purpose other than to evaluate
the proposal; provided, that if a contract is
awarded to this offeror as a result of or in
connection with the submission of such data, the
Government shall have the right to duplicate, use,
or disclose this data to the extent provided in
the contract. This restriction does not limit the
Government's right to use information contained in
such data if it is obtained from another source.

TABLE OF CONTENTS

SECTION I

TECHNICAL PROGRAM

SECTION I

TECHNICAL PROGRAM

This technical proposal presents a program designed to supply, on a time and materials basis over a period of one year, certain technical and scientific services of a staff augmentation nature. The services proposed will lie within the general area of reconnaissance-intelligence technology and will include but not be limited to the following disciplinary areas:

1. Transfer function theory.
2. Wave and geometrical aberration theory.
3. Statistical properties of photographic grain.
4. Evaluation of lens designs.
5. Measurements of optical system performance.
6. Evaluation of Viewers.

The purpose of the proposed program will be to supply technical services at various levels as back-up to the customer's staff. Work undertaken may be independent investigation of problems of customer interest or may be formulated as a continuation of lines of study initiated by the customer.

The work to be pursued under this program will be carried out under mutually agreeable work plans. In

- 2 -

addition to experimentation and analysis performed at
[   ] facility, consulting, advisory   STAT
and/or other services will be supplied to the customer at
his facility and upon his request. It is proposed that
certain lines of investigation be established within thirty
(30) days after contract, such investigative lines being
based upon current problems of customer interest. Such
fields of investigation might include:

     1.   Relations between areal images formed
         by lens systems and the resulting photo-
         graphic image for various films.

     2.   Evaluation of existing optical systems and
         viewers.

     3.   Assistance in fabrication of unusual photo-
         graphic targets and gratings.

    The work proposed will be performed under the direct
supervision of [   ] President, who will act   STAT
as Chief Investigator. [   ] will be assisted by   STAT
[   ] (respectively   STAT
Chief Consultant and Director of Research). Other staff
members will assist as required. A total of 1138 hours
as proposed with engineering and scientific services to
be supplied in the following categories:

- 3 -

Consultant: STAT

Computer Services

Project Manager

Senior Scientist

Scientific Investigator

Staff Engineer

Draftsman

Technician

SECTION II

BACKGROUND AND EXPERIENCE

- 4 -

SECTION II

BACKGROUND AND EXPERIENCE

[   ] is well equipped from   STAT

both facility and personnel standpoints to conduct ex-

perimental and theoretical investigation in all subject

related fields.

The material contained in the following pages

is descriptive of Company experience, staff, and facility.

SECTION II

BACKGROUND AND EXPERIENCE

We have assembled a group of craftsmen, engineers, and physicists whose skill in optics and related fields is unsurpassed.

Our capability encompasses the optical problem from the mathematical theory of lens design and systems analysis, through the modern test facilities necessary for the evaluation of advanced optical hardware.

Our contracts have ranged in value from a few hundred dollars for brief technical consulting tasks, to over one million dollars for the production of high precision optical assemblies. Our projects most often include design and development, as well as manufacture.

We hope that the following synopsis of representative contracts will serve to indicate our range of interest and experience.

A Plant and Facilities list, and appropriate resumes are also included.

STAT

I   ASTRONOMICAL SYSTEMS AND TELESCOPES

1. Design study and fabrication of two complete sets
    of reflecting optics for the N.A.S.A. Goddard Ex-
    perimental Package Orbiting Astronimical Observa-
    tory, each set consisting of one Kanigen coated
    beryllium primary mirror 30 inches in diameter,
    one fused silica secondary mirror 13 inches in
    diameter, one Kanigen coated beryllium spectro-
    meter mirror 23 inches in diameter, and one
    Kanigen coated beryllium grating blank 10 inches
    in diameter, all of which are aspheric, (on the
    order of 100λ except for the grating blank) and
    accurate to $1/4\lambda$.

2. Design, (mechanical) and fabrication of tempera-
    ture insensitive 18 inch aperture $1/4\lambda$ accuracy
    catadioptric telescope.

3. Design and fabrication of 24 inch aperture six
    element Fresnel prism for use with fast Schmidt
    type optical systems. The assembly was made
    from astronomical objective quality glass and
    has resolution accuracies on the order of two
    arc seconds.

4. Design and fabrication of 24 inch aperture Casse-
    grainian Telescope assembly for use in tracking
    operations.

5. Development and fabrication of reflecting optical
    components for astronomical research in the X
    radiation region.

STAT

II   PHOTOGRAPHIC RECONNAISSANCE,
COPYING EQUIPMENT, AND VIEWERS

1. Design, development, and fabrication of a variety of long focal length high acuity aerial reconnaissance lenses, both in prototype and production quantities. These lenses are, in general, diffraction limited and contain multiple aspheric surfaces.

2. Design and manufacture of very high aperture proto-type lenses requiring advances in the state of the art of lens design, and maximum skill in optical fabrication techniques.

3. Design and fabrication of two 400 ℓ/mm near ultra-violet high acuity copying lenses for use in con-tinuous printing. These unusual 12 inch focal length f/2.5 lenses are presently in use in a U.S. Air Force installation.

4. Design and optical fabrication of a wide field, high magnification, high resolution film viewer using new techniques.

5. Design and fabrication of large aperture f/0.88 Schmidt system engineered as integral part of television projection system.

STAT

III   OPTICAL TEST AND CALIBRATION EQUIPMENT

1. Design and fabrication of diffraction limited
    24 inch aperture 240 inch focal length off-axis
    catadioptric collimator for use in testing
    large aperture telescopes on the Atlantic
    Missile Range.

2. Fabrication of high precision 38 inch aperture
    380 inch focal length fused silica Cassegrainian
    optical collimator system.

3. Design and fabrication of 5 inch aperture star
    field simulator with 3 stars having 5 arc second
    size and collimation accuracy, independent
    magnitude variation, and continuous angular
    adjustment.

4. Research and development in the field of optical
    system analysis techniques, including aspects
    relating to photographic film and the photo-
    graphic process.

5. Quantity production, by photography, of high
    resolution test targets having spatial fre-
    quencies up to 1000 ℓ/mm.

STAT

IV   COHERENT OPTICAL SYSTEMS
(prototype and production)

1. Design and fabrication of multi-element optical systems involving the use of ultra-clean $1/8\lambda$ accuracy cylindrical surfaces.

2. Design and fabrication of diffraction limited optical assemblies for 6328 Å light including highly aspheric f/1 components.

Page Denied

Next 3 Page(s) In Document Denied

STAT

PLANT AND FACILITIES

The company occupies a custom designed and constructed 39,000 square foot building on a four acre plot in the Bedford-Burlington research area. Activities in the building include design, research, development and manufacturing; testing areas include a thermally controlled fifteen by seventy-five foot room containing, among other equipment, our master collimator and lens bench mounted on a thirty foot long vibration isolated concrete pad.

Design facilities include the Royal-McBee RPC-4000 computer, standard computer accessories and Monroe desk calculators.

A partial inventory of major laboratory and fabrication equipment includes:

MACHINE SHOP

1   Abrasive Surface Grinder
3   Bridgeport Millers
1   Cincinnati Miller
1   Grob Band Saw
1   Kalamazoo Metal Saw
1   Porter Cable Belt Sander
1   Prentice Lathe
1   Sigma Precision Lathe
1   South Bend Precision Lathe

POLISHING*

2   16" Strasbaugh Polishers (8 spindles)
4   18" Strasbaugh Polishers (16 spindles)
2   16" _____ Polishers   STAT
7   12" _____ Hand Finishing Spindles
1   40" _____ Hand Finishing Spindle
1   _____ Conic Section Generator   STAT
4   50" _____ Triple Motion Polishers   STAT
    (two with aspherizing units)
4   10" Elgin Polishers (16 spindles)
4   26" Loh Double Arm Polishers (two with aspherizing units)
4   6"   _____ Cylindrical Polishers   STAT

ROUGH GRINDING*

1   _____ Diamond Glass Cutting Saw   STAT
1   16" _____ Edger and Grinder   STAT
1   16" _____ Sphere Generator
1   34" _____ Sphere Generator
1   _____ 5 Spindle Edging Machine   STAT
1   Felker Diamond Saw
1   16" Lensmaster Rough Hand Surfacer
1   30" _____ Rough Hand Surfacer   STAT
1   24" Strasbaugh Generating and Edging Machine

*Diameters are nominal: larger sizes can often be accommodated.

STAT

TEST AND ASSEMB

STAT

1 Spectra Physics Model 131 Gas Laser
1 Abbe Refractometer
1 Beckman DU Spectrophotometer
2 Cadillac Height Gages
1 10 foot, .001" Accuracy, Optical Bench   STAT
1 Radius Measuring Bench
1 38" Aperture 1/20λ Optical Flat
1 144" f/8 Parabolic Collimator
2 Aspheric Surface Measuring Devices
1 20" Aperture Test Sphere
1 Barry Controls Vibration Isolation System on Air Mounts
   30' x 4 1/2' x 2'
3 Precision Rotary Tables
1 Nikon Collimator 1/2 second
1 16" Aperture 22' Radius 1/20λ Test Sphere STAT
1 Edcraft Clean Bench
3 Gaertner Laboratory Optical Benches
1 Graf Apsco Binocular Microscope
1 Hilger & Watts Angle Dekkor
1 Perkin-Elmer Infrared Recording Spectrophotometer
4 R.C.A. Air Gages - 10,000:1 amplification
1 Electronic Profile Measuring Gage

PHOTOGRAPHIC LABORATORY

Modern Darkrooms
  Visible and UV Light Sources   STAT
  Vacuum Operating Contact Printer
  Modulation Transfer Test Equipment
  Microdensitometer
Joyce-Loebl, Mark IIIC, Microdensitometer
  Automatic Processing Equipment   STAT
  Emulsion Coating Equipment
B&L Micrographic Camera
  Precision Reduction Camera 1:10   STAT
  Precision Reduction Camera 1:10
  Precision Reduction Camera 1:50
  Precision Reduction Camera 1:100
Kuhlmann Model GM 1/1 Pantograph

OPTICAL COATING FACILITIES

Large Separated Dust Free Area with Special Ventilating and
Cleaning Facilities

1 Edwards High Vacuum Unit with 8" Diameter Bell Jar
1 Bendix Balzer Vacuum Unit with 20" Diameter Bell Jar

The Role of Eikonal and Matrix Methods in Contrast Transfer Calculations

W. Brouwer, E. L. O'Neill, and A. Walther

The Role of Eikonal and Matrix Methods in Contrast Transfer Calculations

W. Brouwer, E. L. O'Neill, and A. Walther

The notion that the optical contrast transfer function is a useful tool for assessing the performance of image-forming instruments has been accepted generally for some time and is now well established. This paper discusses one method of making the transition from ray-trace data to the evaluation of this important function. First, the light distribution in the point image is rigorously derived in terms of an integral over angular coordinates involving the eikonal function about a reference surface at infinity. Then, the ray-trace procedure is developed in the language of refraction and translation matrices culminating in matrix elements which are simply related to the eikonal coefficients of wave optics. Finally, the numerical evaluation of the contrast transfer function in amplitude and phase from these eikonal coefficients is presented, and the paper ends with an example showing the off-axis transfer function for line structures oriented at various azimuths. All calculations are carried out to fifth order in the eikonal coefficients, and emphasis is placed on the usefulness of this approach on relatively slow, low-capacity computing machines.

I. Introduction

The application of Fourier techniques to the theory of image formation has been studied extensively in the preceding decade.

The theory that was developed has been accepted generally as a useful tool in the analysis of optical systems. It centers on two concepts: point-spread function and frequency-transfer function, one being the Fourier transform of the other. Each of these functions can, in principle, be determined when the geometrical aberrations of the lens are known.[1-3]

In practical problems of lens design the ability to evaluate the transfer function numerically would be a great asset to the lens designer. The authors have the impression that one step in the procedure of computing this function is not well known to many workers in the field: the conversion of ray-trace data into wavefront deviations. Following Luneberg[4] and Wolf,[5] we shall treat this problem in a way which is at once simpler and more rigorous, by using eikonal functions instead of wavefront shapes. This approach has the additional advantage that it shows in a unique way the transition from wave optics to geometrical optics.

W. Brouwer and A. Walther are with Diffraction Limited, Inc., Bedford, Massachusetts. E. L. O'Neill is with the Physics Department, Boston University, Boston, Massachusetts.
Received 5 August 1963.

In the ray-tracing calculations a system of two by two matrices as introduced by Smith[6] and Brouwer[7] will be used to great advantage: the relation between the matrix elements and the eikonal functions will be shown to be very simple, and easier to apply than the usual ray intercepts. This leads to a way of calculating the transfer function that is well suited to relatively slow computers with a rather small memory capacity.

In Sec. II we derive an expression for the point-image amplitude distribution using the eikonal function to describe the aberrations and perform a Fourier transformation over the angular coordinates of a reference surface at infinity. In Sec. III we relate the matrix elements determined from geometrical lens design calculations to the eikonal function. Finally, in Sec. IV, starting with the coefficients in the eikonal expansion, we show several examples of off-axis transfer functions using the numerical integration scheme of Hopkins.[8]

II. Transition from Geometrical Wave Optics

A. Notation

We shall have occasion to use four planes associated with a rotationally symmetrical lens [Fig. 1(a)]. These planes are perpendicular to the axis of the lens and are, respectively, the object plane (coordinates x and y), the entrance pupil plane (coordinates x_1 and y_1), the exit pupil plane (coordinates x_1' and y_1'), and

(a)

Entrance
Pupil

Image

(b)
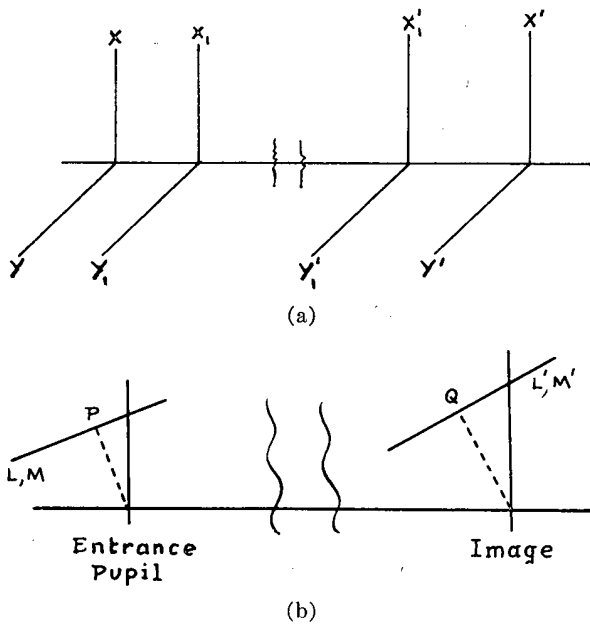
Fig. 1. (a) Coordinate systems. (b) Definition of angle–angle eikonal.

the image plane (coordinates x' and y'). The four axes marked with x lie in one plane, and so do the axes marked with y. The x and y axes are mutually perpendicular and intersect in the axis of the lens, marked by z, z_1, z_1', or z' depending on which of the four planes is used as a reference. The refractive index in the object space is denoted by n; in the image space it is n'. Since we consider only axially symmetric lenses and, unless indicated otherwise, an object point will be understood to lie on the x axis, we are allowed to refer to the x–z plane as the meridional plane.

B. Summary of Fourier Optics

In order to establish our notation and for reference purposes we shall give a brief summary of the basic concepts in Fourier optics. In what follows, $F(x_1',y_1')$ describes the complex scalar disturbance over the exit pupil plane, $a(x',y')$ the complex amplitude distribution in the image of a point source, $s(x',y')$ the intensity-spread function, and finally $D(\nu_x,\nu_y)$ the frequency response or transfer function for the system. By a direct application of Huygen's principle together with approximations that are quite valid for most optical systems it is not difficult to show that $a(x',y')$ and $F(x_1',y_1')$ are Fourier transform pairs in the form

$$a(x', y') = \int\int_{-\infty}^{+\infty} F(\nu_x, \nu_y) \exp\left[2\pi i(\nu_x x' + \nu_y y')\right] d\nu_x d\nu_y, \quad (1)$$

where ν_x and ν_y are reduced coordinates in the exit

pupil about which we shall say more later, and where all constants and the finite area of integration have been absorbed into $F(\nu_x,\nu_y)$. Now by virtue of the fact that we are treating the optical system as a filter of spatial frequencies there exists a further Fourier transformation between $s(x',y')$ and $D(\nu_x,\nu_y)$ in the form

$$D(\nu_x, \nu_y) = \frac{\int\int_{-\infty}^{+\infty} s(x', y') \exp\left[-2\pi i(\nu_x x' + \nu_y y')\right] dx' dy'}{\int\int_{-\infty}^{+\infty} s(x', y') \, dx' dy'}, \quad (2)$$

where the denominator has been introduced for normalization purposes ($|D(0)| = 1$). Capitalizing both on the fact that $s(x',y') = |a(x',y')|^2$ and the convolution theorem for the transform of a product, we end up with a direct relation between the disturbance over the exit pupil and the frequency response in terms of the well-known integral

$$D(\nu_x, \nu_y) = \frac{\int\int_{-\infty}^{+\infty} F(\mu_x, \mu_y)F^*(\mu_x - \nu_x, \mu_y - \nu_y) d\mu_x d\mu_y}{\int\int_{-\infty}^{+\infty} |F(\mu_x, \mu_y)|^2 d\mu_x d\mu_y}. \quad (3)$$

These relations together with their physical interpretations have been fully described in the literature, and the uninitiated reader is invited to consult the references for further details of the Fourier approach (e.g., refs. 2 and 3). As it stands, the phase portion of $F(\mu_x, \mu_y)$ describes a surface of constant phase about a reference sphere passing through the center of the exit pupil whose center is an appropriate point in the image plane. Unfortunately, we have not found this a convenient reference surface in our attempts to bridge the gap between wave optics and geometrical optics. This transition is an important point. We wish to emphasize that the shape of the wavefront can be determined to *any accuracy desired* by means of the laws of geometrical optics. Consequently, any approximation in the translation of these geometrical data to data used in the work on diffraction involves an unnecessary waste of available information. Methods have been suggested to remove the wavefront deformation function from the exponent of the diffraction integral in an artificial manner so as to use quasi-geometrical methods in passing from the exit pupil to the image plane. These techniques (e.g., spot diagrams) must be treated with utmost care; in this paper we shall not take recourse to these approximations.

C. Wavefront Deviations

Our first aim shall be to establish a reasonably exact derivation for Eq. (1), which will automatically lead to the proper definition of ν_x and ν_y. We shall, as is usual in this field, restrict ourselves to the Huygens–Fresnel diffraction theory. There are several undesirable features in the usual derivation of Eq. (1). We mention:

(1) The shape of the wavefront depends on where one choses its location.

(2) Some authors measure the deviation of the wavefront along the rays. Others measure along the radii of the reference sphere.

(3) The relations between the coordinates that define a ray geometrically and the coordinates suited to diffraction calculations are very complicated.

(4) The diffraction integral takes only approximately the form of a Fourier integral.

The approach taken to this problem in the present paper, found to be due to Luneberg,[4] and also treated by Wolf[5] avoids these problems.

In Fig. 2, let $P(x,y)$ be an object point of which an optical system creates a diffraction image in the (not necessarily Gaussian) image plane (x',y'). Let $P'(x_0' + \xi', y_0' + \eta')$ be a point in which we wish to evaluate the amplitude of the diffracted light; ξ' and η' are coordinates in the diffraction pattern, measured in the image plane with respect to a reference point (x_0', y_0') which conventionally is chosen as the intersection point of the principal ray with the image plane.

When the light has traversed the optical system, the pencil of light is completely determined by a wavefront Σ. The line AQ represents a ray in the image space.

The wavefront being a surface of equal phase, the amplitude in the point P' is proportional to:

$$a(P') = \int_{\Sigma} F(A) \exp\left(\frac{2\pi i}{\lambda} W\right) d\sigma, \qquad (4)$$

in which $W = \overline{AP'}$ and $F(A)$ is the amplitude distribution over the wavefront Σ. A discussion of this amplitude distribution in the wavefront is outside the scope of this paper.

Let the direction of rays in the image space be given in terms of their optical direction cosines (L', M', N') which are defined as the geometrical direction cosines multiplied with the refractive index of the image space. Let OS be the normal drawn from the origin in the (x',y') plane onto the ray AQ. Then the optical path length $\overline{PAS}$ considered as a function $E(x,y,L',M')$ of x,y,L', and M' is known as the (point-angle) mixed eikonal of the system.[9,10]

When this function is known, the coordinates (x',y') of the intersection point of a ray with the image plane are given by:

$$\frac{\partial E}{\partial L'} = -x', \frac{\partial E}{\partial M'} = -y', \qquad (5)$$

and the direction cosines of the rays in the object space:

$$\frac{\partial E}{\partial x} = -L, \frac{\partial E}{\partial y} = -M.$$

Let RP' be the normal from P' drawn onto the ray AQ. Then we can write for the path length $\overline{AP'}$ in Eq. (4):

$$\overline{AP'} = E(L', M') - \overline{PA} + \overline{SR} + (\overline{AP'} - \overline{AR}), \qquad (6)$$

in which the dependence of E on x and y is omitted because we assume the object point to be fixed. The path $\overline{PA}$ is constant and may accordingly be dropped. The location of the wavefront is irrelevant, as long as we do not choose it "too close to the image plane." A great simplification is obtained if we make full use of this freedom and move the wavefront out to infinity. In that case the term $(\overline{AP'} - \overline{AR})$ in (6) reduces to zero and the line AP' becomes parallel to the ray AQ. For the projection $\overline{SR}$ of the line OP' onto the ray AQ we can write:

$$\overline{SR} = L'(x_0' + \xi') + M'(y_0' + \eta');$$

consequently, we have:

$$W = E(L,' M') + L'x_0' + M'y_0' + \xi'L' + \eta'M'.$$

A point on the wavefront is now no longer specified by linear coordinates; it must be specified as a direction. So the diffraction integral (1) reduces to:

$$a(P') = \int\int_{\Sigma} \overline{F}(L'M') \exp \frac{2\pi i}{\lambda} [W_0(L',M') + \xi'L' + \eta'M']dL'dM' \qquad (7)$$
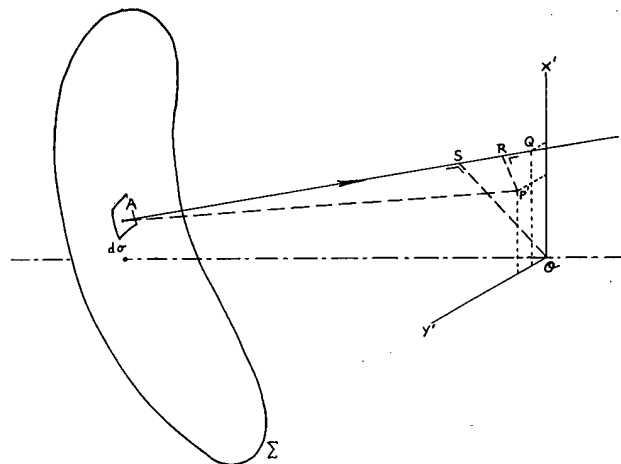

Fig. 2. Wavefront configuration.

in which

$$W_0(L,'M') = E(L,'M') + L'x_0 + M'y_0, \quad (8)$$

a function which is open to easy numerical evaluation, as will be shown subsequently.

Comparing Eqs. (7) and (8) with Eq. (1) we observe first of all that the rather vague concept of wavefront deformation has been replaced by a well-defined eikonal function. We also notice that (7) represents a Fourier transformation, provided that we use as variables in the frequency domain:

$$\nu_x = L'/\lambda,$$
$$\nu_y = M'/\lambda. \quad (9)$$

Every pair of values for ν_x and ν_y defines uniquely a point in the exit pupil. The integration over the exit pupil coordinates is now replaced by an integration over direction cosines in the image space. These direction cosines are a natural product of the ray trace, and, consequently, one does not need the linear exit pupil coordinates at all. Luneberg[4] has shown that the limiting procedure of moving the wavefront to infinity is an essential step in the electromagnetic theory of image formation (see also Wolf[5]).

The amplitude function $\bar{F}(L',M')$ is still unknown and must be determined by external means. It may often be assumed to be constant. (See, however, refs. 11 and 12, in which an object point is assumed that radiates uniformly in all directions.)

Equations (7) and (8) form an ideal bridge between geometrical optics and wave optics. Equation (7) shows that the diffraction integral may be considered as a Fourier transform, even for wide apertures and large field angles. Neither an artificially tipped image plane nor a troublesome reference sphere need be introduced. Equation (7) shows a close relationship between the eikonal functions and diffraction theory. This relationship becomes even more apparent when we apply the method of stationary phase to Eq. (7). For large aberrations, the direction (L',M') contributing most to the amplitude in the point $(x_0' + \xi',y_0'+\eta')$ is found by requiring that the exponent be stationary with respect to L' and M'. This yields:

$$\frac{\partial E}{\partial L'} + x_0' + \xi' = 0,$$

$$\frac{\partial E}{\partial M'} + y_0' + \eta' = 0,$$

which are the exact geometrical relations to be expected. We see that in the diffraction theory of image formation all of geometrical optics remains valid; it is however, elevated into the exponent of the diffraction integral.

III. Numerical Evaluation of the Eikonal

The wave-optics description completed, we turn now to the calculation of the eikonal function. In the conventional ray-tracing procedure it is not feasible to determine the relation between the heights of intersection in the image plane and the pupil coordinates in a closed form. We must sample this function numerically, and, if we wish, then determine intermediate values by interpolation. For the eikonal function we have to apply the same technique, for the same reason. This could be done by path-length computations along the rays traced; however, to attain the desired accuracy a double word-length computation has to be used. With moderately small computers this becomes time-consuming. One can, however, simplify these computations considerably by applying the interpolation not to the eikonal function itself but to its first derivatives with respect to the rotationally invariant variables. In a power series development of the eikonal function a term of a degree n in the linear variables leads to terms of a degree $n - 2$ in the power series of the above-defined first derivative, whence the greater accuracy obtainable. Furthermore, these first derivatives are directly related to matrix elements (obtained from a ray trace), that we shall define presently.

A ray-trace procedure consists in following a ray through an optical system. There are fundamentally two steps involved. At each refracting surface the ray changes direction, and in going from one surface to the next the intersection point of the ray with this next surface has to be found. Let us first describe the refraction of a ray at the ith surface of the system. The coordinates of the point of intersection of the ray with the surface in the space before refraction are denoted by x_i, y_i and by x_i' and y_i' when considered in the space after refraction. The optical direction cosines in these two spaces are denoted by L_i, M_i and L_i' and M_i'. It has been shown that the refraction can be written in the form (see ref. 7):

$$\begin{bmatrix} L_i' \\ x_i' \end{bmatrix} = \begin{bmatrix} 1 & -A_i \\ 0 & 1 \end{bmatrix}\begin{bmatrix} L_i \\ x_i \end{bmatrix} = R_i \begin{bmatrix} L_i \\ x_i \end{bmatrix}$$

and

$$\begin{bmatrix} M_i' \\ y_i' \end{bmatrix} = \begin{bmatrix} 1 & -A_i \\ 0 & 1 \end{bmatrix}\begin{bmatrix} M_i \\ y_i \end{bmatrix} = R_i \begin{bmatrix} M_i \\ y_i \end{bmatrix}, \quad (10)$$

where

$$A_i = \frac{n_i' \cos\varphi_i' - n_i \cos\varphi_i}{r_i}.$$

n and n' are the refractive indices of the media in front and behind the surface, φ_i and φ_i' are the angles of incidence and refraction, and r_i is the subnormal of the refracting surface for the ray considered. For a spherical surface this is the radius itself.

Now, with a similar notation, we can write for the translation to the next surface:
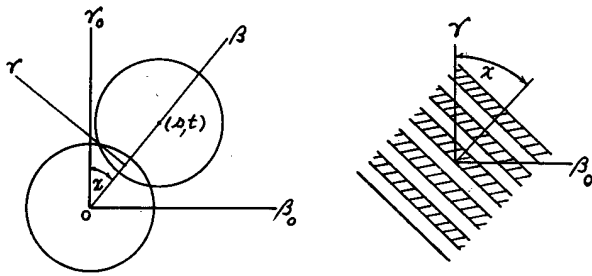
Fig. 3. Rotation of coordinate axes for the computation of the contrast transfer function.

$$\begin{bmatrix} L_{i+1} \\ x_{i+1} \end{bmatrix} = \begin{bmatrix} 1 & 0 \\ T_i' & 1 \end{bmatrix} \begin{bmatrix} L_i' \\ x_i' \end{bmatrix} = T \begin{bmatrix} L_i' \\ x_i' \end{bmatrix}$$

and

$$\begin{bmatrix} M_{i+1} \\ y_{i+1} \end{bmatrix} = \begin{bmatrix} L & 0 \\ T_i' & 1 \end{bmatrix} \begin{bmatrix} M_i' \\ y_i' \end{bmatrix} = T_i \begin{bmatrix} M_i' \\ y_i' \end{bmatrix},$$

(11)

where

$$T_i' = t_i'/n_i.$$

t_i' is the distance measured along the ray between the points x_i', y_i' and x_{i+1}, y_{i+1}. It should be noted that the ray between object point and point of incidence on the first surface can be described by a matrix of the form T and will be denoted by T_0. In the same way in the image space we have a matrix T_n giving the co-ordinates of the ray in the image plane in terms of the coordinates of the ray at the last surface k. When all matrices R_i and T_i are computed the ray coordinates in the image plane in terms of the coordinates of the ray in the object plane can be found by

$$\begin{bmatrix} L' \\ x' \end{bmatrix} = T_k R_k T_{k-1} R_{k-1} \ldots T_2 R_2 T_1 R_1 T_0 \begin{bmatrix} L \\ x \end{bmatrix},$$

and similarly for M' and y as a function of M and y. Since both T and R are 2×2 matrices, the result of the matrix multiplications will be a 2×2 matrix of the form:

$$\begin{bmatrix} L' \\ x' \end{bmatrix} = \begin{bmatrix} B & -A \\ -D & C \end{bmatrix} \begin{bmatrix} L \\ x \end{bmatrix} \quad \text{and} \quad \begin{bmatrix} M' \\ y' \end{bmatrix} = \begin{bmatrix} B & -A \\ -D & C \end{bmatrix} \begin{bmatrix} M \\ y \end{bmatrix}.$$

(12)

Note that the final "x" and "y" matrices are the same; this is due to the rotational symmetry.

Since the optical systems considered here have an axis of symmetry, we can achieve a simplification by introducing the following rotationally invariant quantities:

$$u_1 = \tfrac{1}{2}(x^2 + y^2),$$
$$u_2 = L'x + M'y,$$
(13)
$$u_3 = \tfrac{1}{2}(L'^2 + M'^2).$$

Introducing (13) and (5) into Eq. (12) yields

$$\left(-B\frac{\partial E}{\partial u_1} - A\right)x - \left(B\frac{\partial E}{\partial u_2} + 1\right)L' = 0,$$

$$\left(D\frac{\partial E}{\partial u_1} + C + \frac{\partial E}{\partial u_2}\right)x + \left(D\frac{\partial E}{\partial u_2} + \frac{\partial E}{\partial u_3}\right)L' = 0.$$

Since these relations are valid for all values of x and L' each coefficient should be zero; yielding:

$$\frac{\partial E}{\partial u_1} = -\frac{A}{B},$$

$$\frac{\partial E}{\partial u_2} = -\frac{1}{B},$$
(14)

$$\frac{\partial E}{\partial u_3} = \frac{D}{B},$$

$$BC - AD = +1.$$

Numerical values for these partial derivatives of the eikonal function are thus easily obtained from ray traces. A simple integration will then give the function E.

There are many ways in which this calculation can be performed. In the following a procedure is worked out using truncated power series up to and including the sixth order in the aperture variables to find E as a function of u_2 and u_3, and thus as a function of the co-ordinates L' and M' that we wish to use in the work on diffraction.

Since we are interested only in the function E for one object point, u_1 is a constant and E is a function of u_2 and u_3 only. Let us assume the form

$$E(u_2, u_3) = \Sigma_i \Sigma_j E_{ij} u_2^i u_3^j$$
$$\approx E_{00} + E_{10}u_2 + E_{01}u_3$$
$$+ E_{20}u_2^2 + E_{11}u_2u_3 + E_{02}u_3^2$$
$$+ E_{30}u_2^3 + E_{21}u_2^2u_3 + E_{12}u_2u_3^2 + E_{03}u_3^3$$
$$+ \ldots.$$

(15)

From this it follows that

$$\frac{\partial E}{\partial u_2} = -\frac{1}{B} = E_{10} + 2E_{20}u_2 + E_{11}u_3 + 3E_{30}u_2^2 + 2E_{21}u_2u_3$$
$$+ E_{12}u_3^2 + \ldots,$$

(16)

$$\frac{\partial E}{\partial u_3} = \frac{D}{B} = E_{01} + E_{11}u_2 + 2E_{02}u_3 + E_{21}u_2^2 + 2E_{12}u_2u_3$$
$$+ 3E_{03}u_3^2 + \ldots.$$

All coefficients appearing in the desired function E appear in the functions (16) except E_{00}. However, E_{00} is a constant and therefore not needed in the computations on diffraction. The coefficients E_{ij} in (16) can now be found from the values of the matrix elements B and D for five or more rays. We use a least-

square method where the number of rays used is determined by the desired fit.

It is interesting to note that in this approximation only five meridional rays are needed. The object is situated on the x axis, and so we have for meridional rays:

$$u_2 = L'x,$$

$$u_3 = \tfrac{1}{2} L'^2,$$

and thus:

$$-\frac{1}{B} = E_{10} + (2E_{20}x)L'$$

$$+ (\tfrac{1}{2}E_{11} + 3E_{30}x^2)\, L'^2 + (E_{21}x)L'^3 + \tfrac{1}{4}E_{12}L'^4,$$

$$\frac{D}{B} = E_{01} + (E_{11}x)L' + (E_{02} + E_{21}x^2)L'^2 + (E_{12}x)L'^3 + \tfrac{3}{4}E_{03}L'^4.$$

Five meridional rays, using the first equation gives: E_{10}, E_{20}, $(\tfrac{1}{2}E_{11} + 3E_{30}\, x^2)$, E_{21}, and E_{12}. Four of the same rays, and the second equation gives: E_{01}, E_1, $(E_{02} + E_{21}\, x^2)$, E_{03}. Simple inspection shows that all coefficients can then be computed. When the object is at infinity the same procedures can be used with the help of the angle–angle eikonal as shown in the appendix.

IV. Calculation of the Transfer Function

Having shown the relation between the information supplied by the ray trace (the matrix elements) and the coefficients E_{ij} of the eikonal function we now proceed to calculate the transfer function. In doing so it proves convenient to define normalized variables over which we carry out the numerical integration. Letting L_m' and M_m' represent the maximum* direction cosines as seen from the image field point we now define

$$\beta_0 = L'/L'_m \text{ and } \gamma_0 = M'/M_m'.$$

Further, we define normalized polar coordinates $\beta_0 = \rho \cos\phi$; $\gamma_0 = \rho \sin\phi$ such that $0 \le \rho \le 1$ and we see that aside from scale factors which can be absorbed into the coefficients, u_2 can be replaced by β_0 and u_3 by ρ^2. We now can write the basic integral for the evaluation of the transfer function in terms of these normalized variables as:

$$D(s, t) = \frac{\displaystyle\int\!\!\int_{-\infty}^{\infty} F(\beta_0, \gamma_0)F^*(\beta_0 - s, \gamma_0 - t)\, d\beta_0 d\gamma_0}{\displaystyle\int\!\!\int_{-\infty}^{\infty} |F_0(\beta_0, \gamma_0)|^2\, d\beta_0 d\gamma_0}, \quad (17)$$

where s and t are line frequencies normalized such that they run from 0 to 1, and where for our purposes we take

---

* Actually L_m' and M_m' are symmetrized forms of the direction cosines that limiting rays make with the x', y' axes as seen from an off-axis field point.

$$F(\beta_0, \gamma_0) = \exp\left[\frac{2\pi i}{\lambda}E(\beta_0, \gamma_0)\right], \quad \beta_0{}^2 + \gamma_0{}^2 \le 1$$

$$= 0, \qquad \beta_0{}^2 + \gamma_0{}^2 > 1.$$

Finally, for ease in computation it turns out to be convenient to perform a translation and rotation of axes to β, γ centered at the common area of the displaced circles* such that β points along the direction of the normal (ψ) of the line structure in the object plane (see Fig. 3). With these changes of variables our basic integral can be cast into the form:

$$D(s, \psi) = \frac{\displaystyle\int\!\!\int_{-\infty}^{\infty} F\left(\beta + \frac{s}{2}, \gamma\right)F^*\left(\beta - \frac{s}{2}, \gamma\right)d\beta d\gamma}{\displaystyle\int\!\!\int_{-\infty}^{\infty} |F(\beta, \gamma)|^2 d\beta d\gamma}. \quad (18)$$

At this point we adopt the numerical integration scheme of Hopkins[8] and write first

$$D(s, \psi) = \frac{1}{a}\int\!\!\int_{\infty} \exp\left[iksV(\beta, \gamma; \psi)\right]\, d\beta d\gamma, \quad (19)$$

where $a = \int\!\int d\beta d\gamma$ is the normalization constant and $V(\beta, \gamma; \psi)$ is given by:

$$V(\beta, \alpha; \psi) = \frac{1}{s}\left[E\left(\beta + \frac{s}{2}, \gamma; \psi\right) - E\left(\beta - \frac{s}{2}, \gamma; \psi\right)\right] \quad (20)$$

$$= \frac{\partial E}{\partial \beta} + \frac{1}{3!}\left(\frac{s}{2}\right)^2\frac{\partial^3 E}{\partial \beta^3} + \frac{1}{5!}\left(\frac{s}{2}\right)^4\frac{\partial^5 E}{\partial \beta^5}.$$

Now as Hopkins[8] has demonstrated (see also Marchand and Phillips[13]) this integral can be approximated by a double summation taken over all the elementary cells (ϵ_x, ϵ_y) that fall within the common area in the form

$$D(s, \psi) = \frac{1}{N}\Sigma_m\Sigma_n e^{iZ}\frac{\sin X}{X}\frac{\sin Y}{Y}, \quad (21)$$

where $N = a/(4\epsilon_x\epsilon_y)$ is the number of rectangles of area $4\epsilon_x\epsilon_y$ that fall within the full area a and where

$$X = \epsilon_x ks\frac{\partial V}{\partial \beta},$$

$$Y = \epsilon_y ks\frac{\partial V}{\partial \alpha}, \quad (22)$$

$$Z = ksV(\beta, \gamma; \psi),$$

each of which is evaluated at the center of the elementary cells. Finally, to complete this description we note that we can also write $D(s, \psi)$ in the form

$$D(s, \psi) = |D(s, \psi)|e^{i\theta(s,\psi)}, \quad (23)$$

---

* In actual practice as one gets off-axis the region of integration is the common area of two displaced ellipses. Further, the effect of vignetting must be taken into consideration.
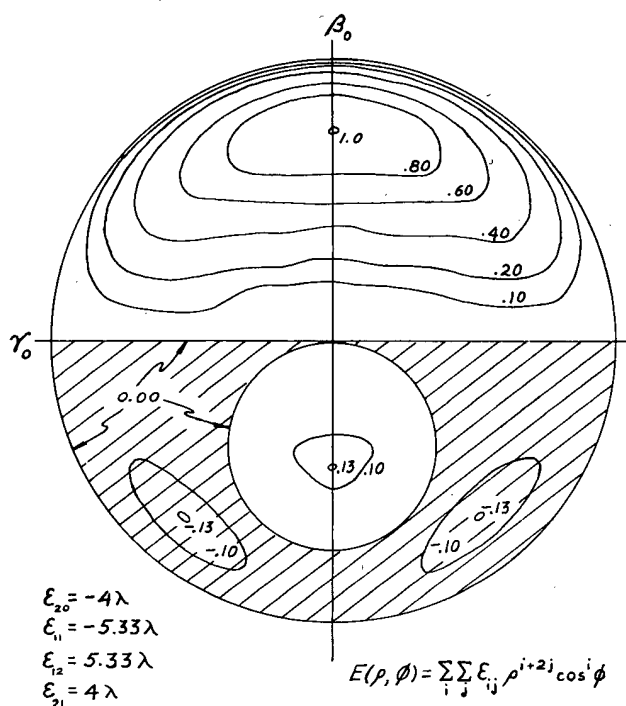
Fig. 4. Rough sketch of normalized wave deformation.

$$\mathcal{E}_{20} = -4\lambda$$
$$\mathcal{E}_{11} = -5.33\lambda$$
$$\mathcal{E}_{12} = 5.33\lambda$$
$$\mathcal{E}_{21} = 4\lambda$$

$$E(\rho, \phi) = \sum_i \sum_j \mathcal{E}_{ij} \rho^{i+2j} \cos^i \phi$$

For our purposes we find the RPC 4000, a relatively modest computer, perfectly adequate. A complete curve, yielding 20 equally spaced points for the amplitude and 20 points for the phase takes $4\frac{1}{2}$ hr. Often the amplitude falls off and remains below a physically meaningful value before the run is completed, and the computer is instructed to proceed directly to the next case of physical interest. These remarks are not meant to minimize the advantages of high-speed computers in optical design. The point we wish to make here is simply that the transfer function is not an end in itself but merely the most useful tool we have to date to assess the relative merits of one design over another. As such this function becomes useful only during the final stages of design after earlier attempts have been rejected for practical and other reasons. Having reached the point where one wishes now to concentrate on a few critical cases, the assessment using the contrast transfer function comes into play, and we here merely wish to emphasize that such evaluations are well within the scope of the more modest computers.

We should like to close this section by giving a numerical illustration for a wave deformation often encountered in practice. Figure 4 shows a wave deformation exhibiting a typical "bubble" along the meridional section as seen from an off-axis field point. On axis all coefficients are zero, and the now familiar transfer function for this case is shown in Fig. 5. Off axis the situation is different, and we show in Fig. 5 the amplitude and phase of the contrast transfer function for line structures whose normals point along the sagittal and meridional section and at 45° to these. Needless to say we find such curves quite useful in evaluating the performance of optical systems.

where

$$|D(s, \psi)|^2 = D_R{}^2(s, \psi) + D_I{}^2(s, \psi),$$

$$\theta(s, \psi) = \tan^{-1} D_I/D_R,$$

and where

$$D_R(s, \psi) = \frac{1}{N} \Sigma_m \Sigma_n \cos Z \frac{\sin X}{X} \frac{\sin Y}{Y},$$

$$D_I(s, \psi) = \frac{1}{N} \Sigma_m \Sigma_n \sin Z \frac{\sin X}{X} \frac{\sin Y}{Y}.$$

It is to be noted in this approach that X, Y, and Z depend upon $V(\beta, \gamma; \psi)$ which in turn depends upon $E(\beta, \alpha; \psi)$. We have found it convenient to express $E(\beta, \alpha; \psi)$ in the form

$$E(\beta, \alpha; \psi) = \sum_{k,l=0}^{k+l \le 6} A_{kl}(\psi) \beta^k \gamma^l, \qquad (24)$$

where the original eikonal coefficients and the orientation of the line structure have been absorbed into the 49 matrix elements A_{kl} (of which 25 are zero in fifth-order theory). As Marchand and Phillips have pointed out, the extension of Hopkins' method to fifth order is a straightforward problem in numerical integration. It is our experience also that a cell size of 0.05 units is sufficiently accurate for all purposes encountered in practice. Moreover, this approach does not necessarily require a high-speed, large-capacity computer.
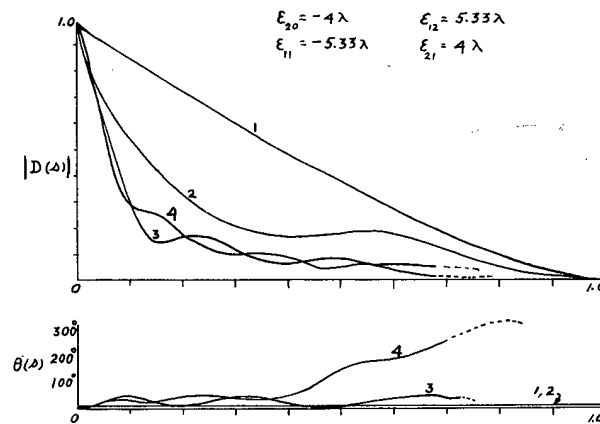

Fig. 5. Contrast transfer functions for wave deformation shown in Fig. 4 at several azimuth angles. Curve 1—on-axis; curve 2—off-axis $\psi = 0$; curve 3—off-axis $\psi = \pi/4$; curve 4—off-axis $\psi = \pi/2$.

We wish to express our gratitude to S. Daniels and H. Sijgers for their roles in bringing this paper to completion.

Appendix

In the case that the object is at infinity it is convenient to use a slightly different eikonal function, the so called angle–angle eikonal.

From the center of the entrance pupil we construct a perpendicular to the ray considered. (See Fig. 1.) The same is done in the object plane. The eikonal is now the optical path length P between the footpoints of these perpendiculars and is a function of $L, L', M,$ and M'.

For a given point at infinity L and M are constants and all points P for rays from this object point are on one wavefront. For this eikonal the following relations hold (see ref. 9)

$$x = \frac{\partial E}{\partial L}, \quad -x' = \frac{\partial E}{\partial L'},$$

$$y = \frac{\partial E}{\partial M}, \quad -y' = \frac{\partial E}{\partial M'}.$$

For rotational symmetric systems the following rotationally invariant quantities are introduced

$$\bar{u}_1 = \tfrac{1}{2}(L^2 + M^2),$$

$$\bar{u}_2 = LL' + MM',$$

$$\bar{u}_3 = \tfrac{1}{2}(L'^2 + M'^2).$$

From this it is easily derived that

$$\frac{\partial E}{\partial \bar{u}_1} = \frac{B}{A},$$

$$\frac{\partial E}{\partial \bar{u}_2} = -\frac{1}{A},$$

$$\frac{\partial E}{\partial \bar{u}_3} = \frac{C}{A},$$

$$BC - AD = +1.$$

All other computations are the same as in the case with a finite object distance.

References

1. B. R. A. Nijboer, thesis, Groningen (1942).
2. M. Born and E. Wolf, *Principles of Optics* (Pergamon Press, London, 1959).
3. E. L. O'Neill, *Introduction to Statistical Optics* (Addison-Wesley, Reading, Mass., 1963).
4. R. K. Luneberg, Lecture Notes, Brown University, Providence (1944).
5. E. Wolf, Proc. Roy Soc., A, *253*, 349 (1959).
6. T. Smith, *A Dictionary of Applied Physics*, R. T. Glazebrook, ed. (Macmillan, London, 1923), Vol. IV, p. 287.
7. W. Brouwer, *Matrix Methods in Optical Instrument Design* (Benjamin, to be published).
8. H. H. Hopkins, Proc. Phys. Soc., London **B70** 1002, 1162 (1957).
9. J. L. Synge, *Geometrical Optics, An Introduction to Hamilton's Method* (Cambridge Univ. Press, New York, 1937).
10. M. Herzberger, *Strahlen Optik* (Springer, Berlin, 1932).
11. H. Osterberg and R. A. McDonald, "Symposium on Optical Image Evaluation," NBS Circ. **526** (1954).
12. R. Barakat and D. Lev, J. Opt. Soc. Am. **53**, 324 (1963).
13. E. Marchand and R. Phillips, Appl. Opt. **2**, 359 (1963).

Technical Note TN100-2

Notes on the Design and Manufacture of
High Precision Cylindrical Lens Systems

STAT

STAT

January 1966

The use of cylindrical lenses in situations where
optical accuracies are important has been known
for some time, as in anamorphic projection sys-
tems, and more recently, in devices related to
spatial filtering. This end of the optical sys-
tem spectrum is continuously pushing into areas
where the ultimate in performance is required,
where the phase characteristics of the wavefronts
must be controlled to more than usual accuracies.

In response to these needs, advanced techniques
for the design and fabrication of systems contain-
ing precision cylinder lenses have been developed.

Design Considerations

_____ has developed its own computer   STAT
programs for the handling of the rather unusual
case of multiple cylindrical elements. The geo-
metry of the meridional ray trace for a cylindrical
surface is, of course, identical to that for a
spherical surface; special treatment is required,
however, for all other planes except for the saggi-
tal plane, where the radius becomes infinite, (or,
in the case of a toroidal surface, a different
radius). Lenses of shape similar to cylinders or
toroids, but whose sections are not circular, have
also been treated, ("acylindrical").

Another consideration in the mathematical analysis
of cylindrical lens systems is the added parameter
of the effect of the rotation of individual elements
or groups of elements. In a rotationally symmetri-
cal system, of course, the formulations are invariant
for rotations of a plane about the optical axis;
this is not true for a cylindrical system, and rota-
tion produces effects on scale and image quality.
We have found paragraphs 33 through 36 of Chapter IV
of Luneburg's excellent book, "Mathematical Theory
of Optics" (Univeristy Press) of invaluable assis-
tance in developing this type of analysis.

We include here an analytical treatment of small rotational errors in cylindrical optics.

When, in a cylinder system, a number of surfaces are close together, such as in a cemented or uncemented "thin" doublet, the effect of slight rotational errors on the shape of the emerging wavefront can be calculated fairly easily.

Let z be the optical axis of a cylinder surface, and y its cylinder axis. Then we can write in a first approximation:

$$z = 1/2Rx^2$$

Let this surface now be, inadvertently, rotated over a small angle ϕ around the z axis.

Then the rotated surface is given by:

$$z_1 = 1/2R(x \cos\phi - y \sin\phi)^2$$

The error introduced in the wavefront may then, for all practical purposes, be considered as being due to the sag difference $z_1 - z = \Delta z$:

$$\Delta z = 1/2R(x \cos\phi - y \sin\phi)^2 - 1/2Rx^2,$$
or, because ϕ is considered small:

$$\Delta z = (-Rxy)\phi + 1/2R(y^2-x^2)\phi^2$$

Let n and n^1 be the refractive indices before and after the surface. If we allow a maximum wavefront deformation of λ/N we then have:

$$\left| (n^1-n)\Delta z \right| < \lambda/N$$

This puts an upper limit on the allowable rotation error ϕ.

-2-

If we use the term linear in ϕ to find this tolerance, the requirements usually become exceedingly tight. There are, however, many cases in which the linear term is compensated for in the final assembly.

As an example we may take the case of an uncemented doublet. If each of the elements has some small rotational error due to imperfections in the fabrication, the effect of these errors can be eliminated in the assembly by properly rotating one element with respect to the other. This technique works for the term linear in ϕ because we can control the sign of ϕ. For the second term a technique of this type is not likely to work because we cannot control the sign of ϕ^2.

Assuming that the diameter of the lens is d, the wavefront aberration due to the second term is

$$1/8 (n^1-n) Rd^2 \phi^2$$

$$= (n^1-n) z_{edge} \cdot \phi^2,$$

in which z_{edge} is the sag of the surface measured at the edge.

Hence the tolerance on rotational errors follows from

$$\phi^2 = \frac{1}{n^1-n} \frac{\lambda}{z_{edge}} \cdot \frac{1}{N},$$

provided that the linear term can be eliminated, and that the cylindrical surfaces are sufficiently close together.

Manufacturing Considerations

Among the systems we have designed, built, and tested, two have combined unusual complexity with extremely high wavefront accuracy requirements. Both had moderate field of view with corrected components working at apertures of approximately f/3. One system contained 24 cylindrical and 24 spherical surfaces; the other contained 8 cylindrical and 18 spherical surfaces. The accuracy requirement in both cases was a diffraction limited imaging capability for the whole system over the field. Maximum apertures were on the order of two inches, and multiple units were fabricated. We have also made a wide variety of similar and very accurate cylindrical systems including diffraction limited cylindrical doublets with apertures of two and one half by eight inches.

Figure 1 shows the diffraction pattern obtained at an anastigmatic focus through one of these complex cylindrical systems. The shape of the pattern is due to the noncircular configuration of the system aperture.

Much thought, experimentation, development, and finally, special equipment construction has been necessary to arrive at the point where consistant and efficient manufacture of $1/8\lambda$ accuracy well centered cylindrical elements is possible.

In the manufacturing of a spherical surface the skilled optician must be able to take advantage of many degrees of freedom in his polishing machine in order to achieve a high precision surface. It is relatively easy to construct such a machine, and in fact, a certain lack of mechanical precision is considered to be beneficial in statistically averaging out possible systematic errors.

-4-

These degrees of freedom are likewise necessary
to the operator of the cylinder polishing machine
with an important and difficult exception. In
the following discussion, the z axis is that per-
pendicular to the optical surface.

The machine must provide independently adjustable
motions and speeds along the x and y axes and
permit free motion along the z axis. It must
also permit free rotation about x and y axes, at
the same time allowing none about the z axis.

The ability of the machine to do this, as well
as the skill of the optician, will determine
the ultimate accuracy that can be attained.

We have designed and built machinery especially
for this purpose, making use of adjustable
hydraulic drives to achieve the multitude and
range of smooth motion required.

Figure 2 shows two views of one of these machines.
Figure 3 shows fringe patterns on two final edged
cylindrical elements as they are tested against
their respective test plates.

Another important manufacturing consideration
is the special wedge and surface alignment prob-
lem involved. In principle, with the limiting
cases such as lenses with no edge thickness,
lenses with radii approaching infinity, and con-
centric lenses, a lens with two spherical sur-
faces can be centered in a mechanical edging
process after the polishing has been completed,
and the optician can pay a minimum attention to
this problem while polishing and figuring the
surface.

Because of the lack of rotational symmetry, the
geometrical relationship between the surfaces
of a cylindrical lens must be held within close
limits during polishing.

The simplest cylindrical lens contains one plane surface. In this case the only concern is lens thickness and wedge, (tilt between cylindrical axis and the plane surface). This must be corrected during the grinding of the plane surface. Wedge in the other direction, (in the direction of curvature) can be removed later.

The most difficult lenses are those having two cylindrical surfaces. During the grinding and polishing of the second surface any twist between the cylindrical axes must be measured as well as wedge. This twist shows up only as a second order effect and must be measured by very precise mechanical techniques. We have employed differential air gage techniques as a means of determining this error, and the lens is twisted an equal amount on the machine to correct it.

Similar methods are used to position the lens for final edging.

A special measuring set up has been developed, capable of measuring errors of fractions of a ten thousandth of an inch, to make the achievement of essentially wedge free cylindrical lenses possible. An illustration of one of these devices is shown in Figure 4.

Although the process is more difficult, and the results more costly than in the use of spherical lenses, our experience indicates that the production of cylindrical lenses of moderate size with surface accuracies on the order of 1/4 to 1/8 λ is feasable in substantial quantities, and that ultimately, accuracies similar to those attainable for spherical surfaces can be realized.
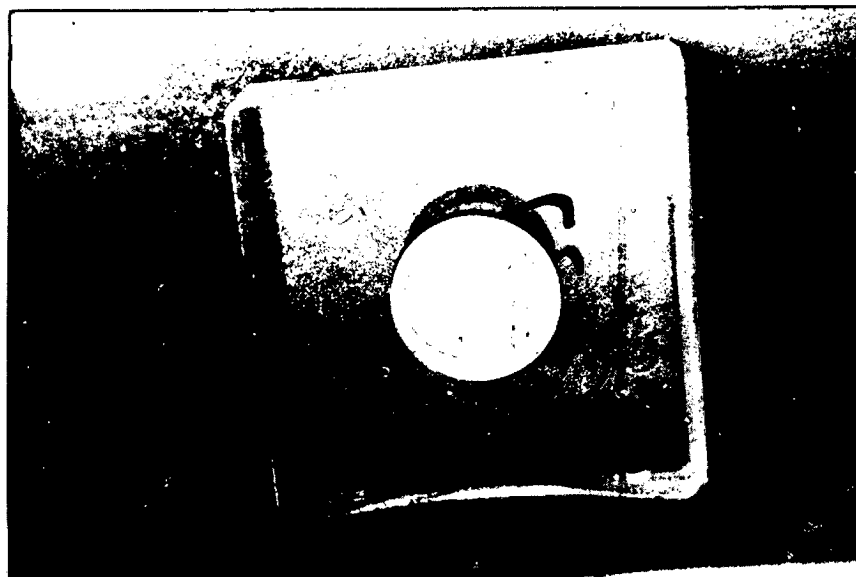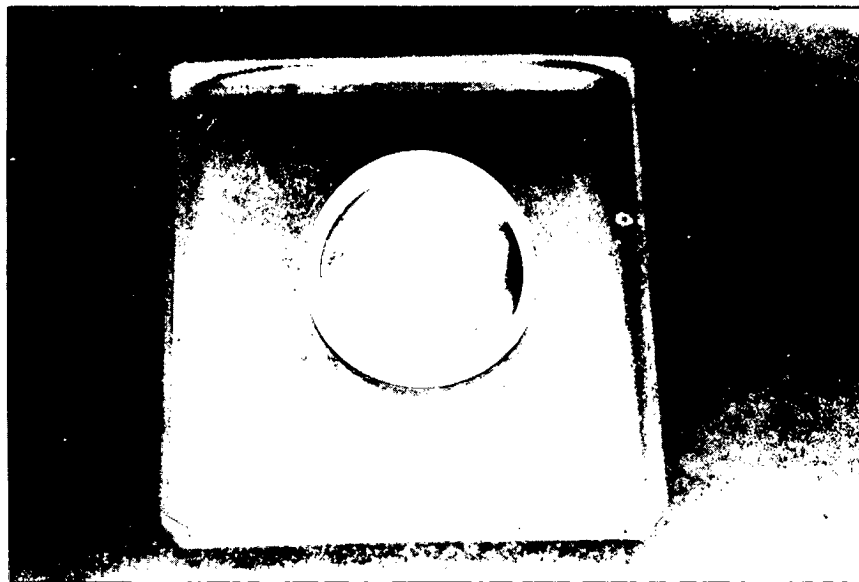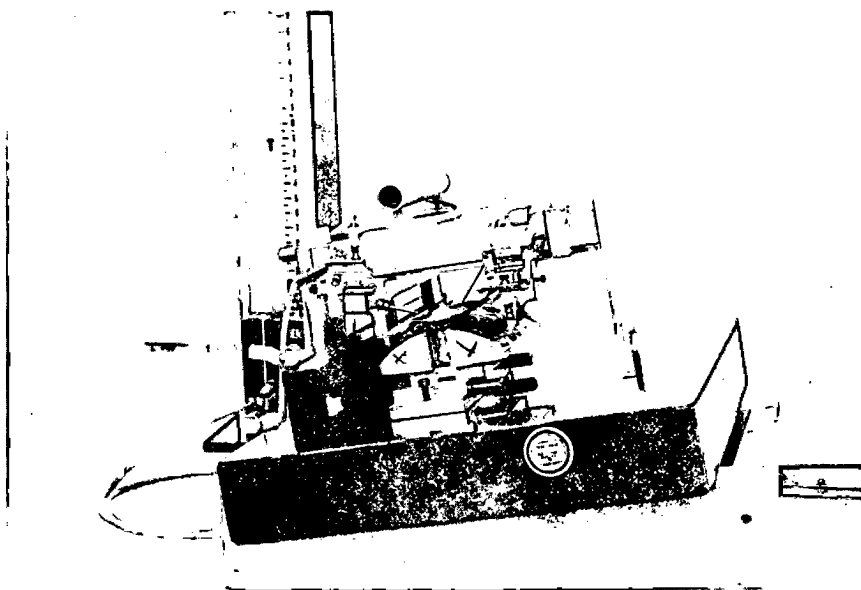
Figure 1
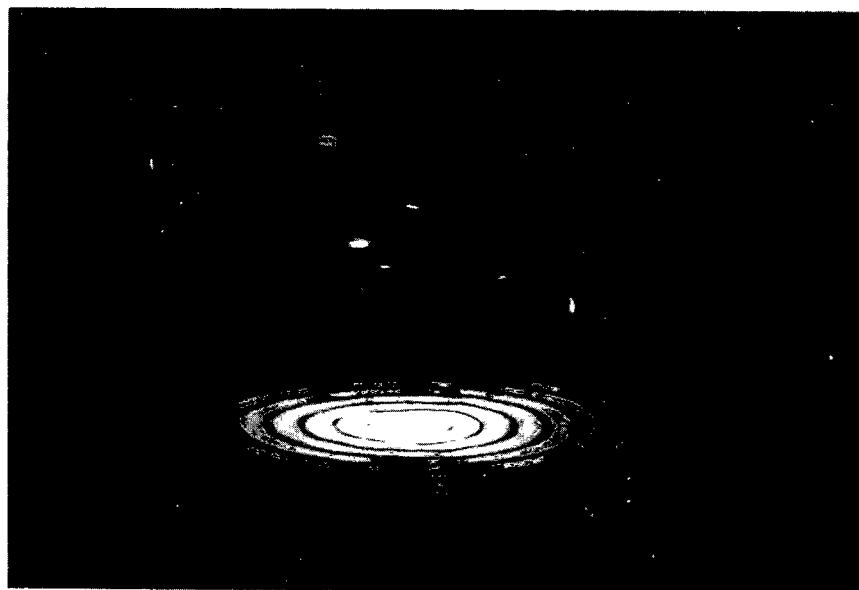
TN100-2

Figure 2

TN100-2

-8-

Figure 3

TN100-2

-9-
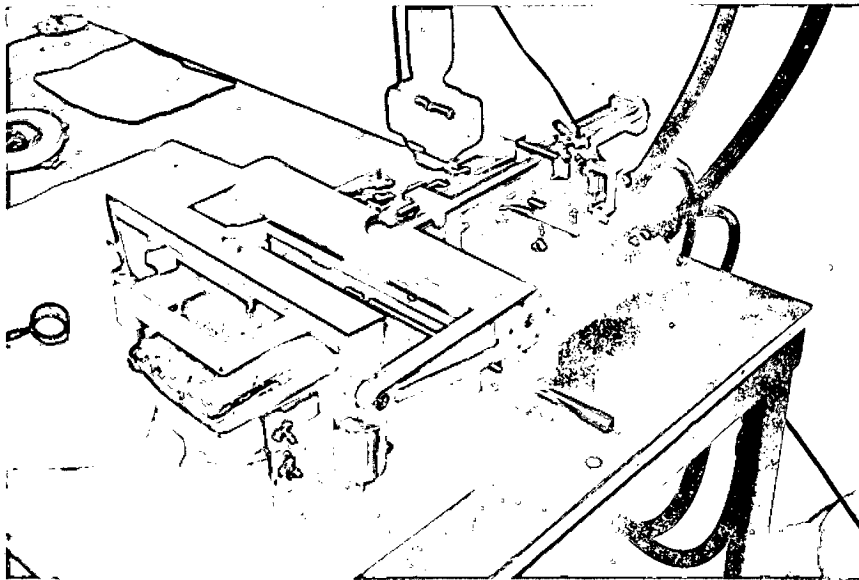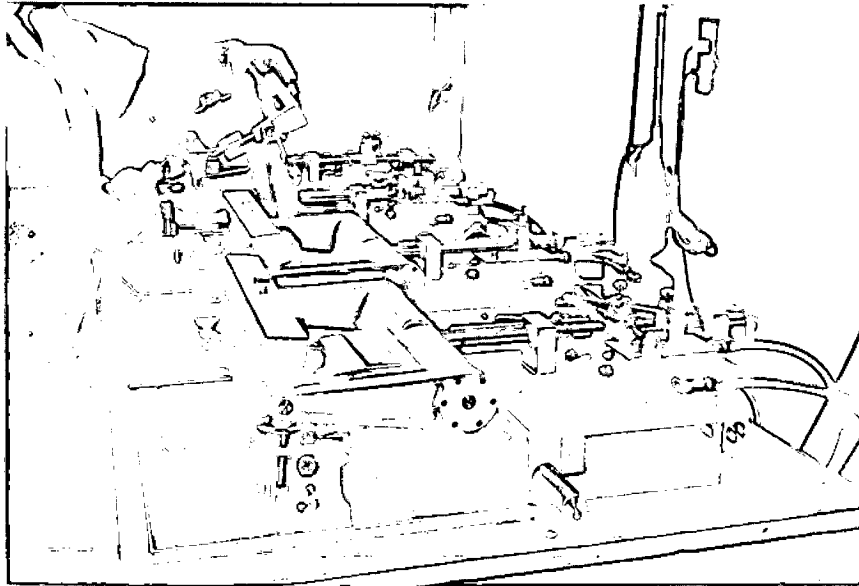
Figure 4

TN100-2

SECTION III

COST DATA

Page Denied